IOSR Journal of Environmental Science, Toxicology and Food Technology (IOSR-JESTFT)
e-ISSN: 2319-2402,p- ISSN: 2319-2399.Volume 11, Issue 4 Ver. II (April. 2017), PP 18-30
www.iosrjournals.org

Adsorption Isotherm Models for Dye Removal by *Paliurus spina-christi* Mill. Frutis and Seeds in a Single Component System

Ali Savran[1], Nilüfer Çiriğ Selçuk[2], Şenol Kubilay[1] , Ali Rıza Kul[1]
[1]*Chemistry Department, Science Faculty, University of YYU, Turkey*
[2]*Biology Department, Science Faculty, University of YYU, Turkey*

Abstract: *This article describes the adsorption of an cationic dye, namely methlene blue (MB), from aqueous solutions onto Paliurus spina-christi Mill. frutis and seeds (PSCFS) adsorbent. Batch equilibrium experiments were conducted to study the effects of contact time, initial pH, initial concentration of MB. The results show that the equilibrium was achieved at 260 min contact time. Equilibrium adsorption isotherms were measured for the single component system and the experimental data were analyzed by using Langmuir, Freundlich, DKR, Temkin, BET, Harkins-Jura, Elovich, Fowler-Gugenheim, Hill de Boer, Frumkin, Halsey, Henderson, Smith, Jovanovic and Scatchard isotherm equations.*

Keywords: *Adsorption, equilibrium, isotherms, methlene blue*

I. Introduction

Water pollution is one of the most serious environmental problems being faced by modern society [1]. MB, one of the dyes forming this pollution, is the most commonly used substance for dying cotton, wood and silk. It can cause eye burns which may be responsible for permanent injury to the eyes of human and animals. On inhalation, it can give rise to short periods of rapid or difficult breathing while ingestion through the mouth produces a burning sensation and may cause nausea, vomiting, profuse sweating, mental confusion and methemoglobinemia [2, 3]. Therefore, the treatment of effluent containing such dye is of interest due to its harmful impacts on receiving waters. Various techniques are in use for the removal of dye from water discharge. Amongst the numerous techniques, adsorption utilizes the ability to accumulate dye from wastewater and gives the best results as it can be used to remove different types of coloring materials[4, 5].

Natural materials have excellent potential as inexpensive adsorbents. Many natural adsorbents have been used in past years for dye removal however, the exploration and development of new adsorbents is endless. In recent years, natural adsorbents such as cucumber peels [6], meranti sawdust[7], bagasse [8], durian leaf powder [9], water melon seed hulls [6], grape pulp [10], chitosan [11], kenaf core fibers [12], sugar beet pulp [13], fly ash generated from coal [14], activated carbon prepared from papyrus plant [15], corn wastes [16], etc. have also been utilized for the removal of methylene blue from aqueous solution.

Paliurus spina-christi is a small tree species that lose their leaves seasonally and growing 3-4 m. This tree is a species of native to the Mediterranean. The leaves are oval, 2-5 cm long and 1-4 cm broad, glossy green, with an entire margin. The fruit is a dry woody nutlet centred in a circular wing 2-3.5 cm diameter. (From Wikipedia). The purpose of this work is to determine the adsorption capacity of natural *Paliurus spina-christi* frutis and seeds (PSCFS). The experiments were carried out using aqueous solutions of methylene blue (MB) at natural pH and investigated adsorption isotherms.

II. Materials and methods

2.1 Dye characterization

MB was chosen for this study because of its known strong adsorptive compound onto materials. Methylene blue (chemical formula: $C_{16}H_{18}ClN_3S$; molecular weight =319.86 g/mol; maximum wavelength = 662 nm) supplied by Merck was used as adsorbate and was not purified prior to use. A stock solution of methylene blue of 1000 mg/L was prepared, which was diluted to the required initial concentrations. Other chemicals were obtained from Merck.

2.2 *Paliurus spina-christi* frutis and seeds (PSCFS)

PSCFS were obtained from local area. The collected materials were then washed several times with distilled water to remove all dirt particulate. The washed materials were then dried in a hot oven at 55 ^{o}C for 24 h.The dried materials were then ground , using a mill. The adsorbent was sieved through 0.06 mm sieve and used without any pretreatment.

2.3 Experimental run

The stock solution of methylene blue (1000 mg/L) was prepared and suitably diluted to the required initial concentrations(20–50 mg/L). The experiment were carried out in 1500 mL beaker containing 100 mL of synthetic dye solution. The effect of the contact time on the amount dye adsorbed was investigated at different initial concentration of dye (20, 30, 40 and 50 mg/L) at different temperatures (298 K, 308 K and 318 K). 4.0 g PSCFS were mixed with 1000 mL dye solutions at different concentrations, natural pH and desired temperatures at 150 rpm for specific time intervals. At the end of the adsorption process, the solution was centrifuged for 10 min at 3000 rpm. After centrifugation, the dye concentration in the supernatant solution was analyzed using a UV spectrophotometer (T80+ UV/Vis) by monitoring the absorbance changes at a wavelength of maximum absorbance (662 nm).

The amount of dye adsorbed was calculated using the equation:

$$q_e = \frac{(C_o - C_e)V}{W} \tag{1}$$

where q_e is the amount adsorbed per gram of adsorbent, C_e is the equilibrium concentration of dye (mg/L), W is mass of adsorbent (g) and V is volume of solutions.

III. Results and discussion

3.1 Effect of initial dye concentrations

The initial concentration provides an important driving force to overcome all mass transfer resistances of the dye between the aqueous and solid phases. The effect of concentration on contact time was also investigated as a function of initial dye concentration. The adsorption of dye by PSCFS were studied at several different initial methylene blue concentrations ranging from 20 to 50 mg/L. The results are shown in Fig. 1.

The results indicate that the rate of dye removal increased depending on the contact time. For PSCFS adsorbent, the amount of adsorbed dye is extremely rapid in the first 90 min. Then the rate of adsorption became slow in the adsorption processes. As can be seen in Figs. 1, when the initial dye concentration was increased, adsorption efficiency increased. But the precentage of adsorption is decreasing. This was due to the saturation of the sorption sites on the adsorbents as the concentration of the dye increased. The equilibrium adsorption capacity of the adsorbent increased with increasing initial dye concentration up to 50 mg/L, while precentage removal of dye showed the opposite trend. When the initial dye concentration increased from 20 mg/L to 500 mg/L, the adsorption capacity of PSCFS increased from 3.83 mg/g to 8.45 mg/g and the adsorption removal for PSCFS decreased from % 76.7 to % 67.6.

3.2 Adsorption isotherms

The data obtained from adsorption equilibrium studies were analyzed according to Langmuir, Freundlich, DKR, Temkin, BET, Harkins-Jura, Elovich, Fowler-Gugenheim, Hill de Boer, Frumkin, Halsey, Henderson, Smith, Jovanovic and Scatchard isotherm equations. These isotherm equations are commonly used to describe adsorption at specified temperatures for water and wastewater treatment applications.

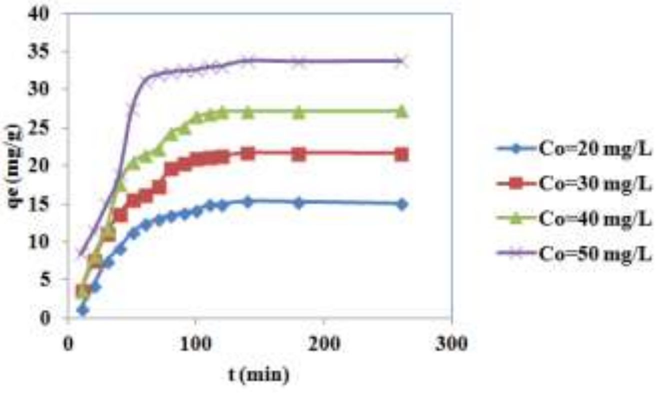

Fig. 1. Effect of contact time and initial dye concentration on dye removal. PSCFS dose 4 g/L (natural initial pH, at 298 K, agitation speed 150 rpm).

The Langmuir model is valid for monolayer sorption onto a surface with a finite number of identical sites. The distribution of dyes between the solid solution interface equilibrium has been described by the

Langmuir equation [17]. Langmuir isotherm was the most commonly used linear expression to study the relation between the concentration of solute in liquid phase and in the solid phase at equilibrium conditions[18]. The well known expression of the Langmuir model is given as:

$$\frac{1}{q_e} = \frac{1}{q_m K_L C_e} + \frac{1}{q_m} \qquad \textbf{(2)}$$

Where *qe* (mg/g) and *Ce* (mg/L) are the amounts of adsorbed dye per unit weight of adsorbent and unadsorbed dye concentration in solution at equilibrium, respectively. q_m*(mg/g)* and K_L*(L/mg)* are the Langmuir constants, representing the maximum adsorption capacity for the solid phase loading and the energy constant related to the heat of adsorption respectively. The essential characteristics of the Langmuir isotherm can be expressed by a dimensionless constant called equilibrium parameter, R_L defined by[19]:

$$R_L = \frac{1}{1+K_L C_o} \qquad \textbf{(3)}$$

where K_L is the Langmuir constant and C_0 is the initial dye concentration (mg/L), R_L values indicate the type of isotherm [20]. R_L value indicates the adsorption nature to be either unfavourable ($R_L > 1$), linear ($R_L = 1$), favourable ($0 < R_L < 1$) or irreversible ($R_L = 0$).

Langmuir parameters were obtained from the linear correlations between the values of $1/q_e$ *and* $1/C_e$ (Fig. 2) and these parameters are shown in Table 1. The R^2 values suggest that the Langmuir isotherm provides a good model of the sorption system. This indicates the applicability of adsorption isotherm and the monolayer coverage on the adsorbent surface. According to Langmuir isotherms, the maximum amount of dye per unit weight of adsorbent was 21.692 mg/g in this study (at 318 K). The R_L values are found in the range of 0.251-0.455, 0.187–0.365 and 0.244–0446 for methylene blue at 298, 308 and 318 K, respectively, showing favorable adsorption. Freundlich isotherm is the earliest known relationship describing the non-ideal and reversible adsorption, not restricted to the formation of monolayer and demonstrated that the ratio of the amount of solute adsorbed onto a given mass of adsorbent to the concentration of the solute in the solution was not a constant at different solution concentrations [21]. This empirical model can be applied to multilayer adsorption, with non-uniform distribution of adsorption heat and affinities over the heterogeneous surface [22]. The emprical Freundlich equation based on sorption onto a heterogeneous surface is given as:

$$q_e = K_F C_e^{1/n} \qquad \textbf{(4)}$$

Eq.(5) can be rearranged to obtain a linear form by taking logarithms Eq.(4):

$$\ln q_e = \ln K_F + \frac{1}{n}\ln C_e \qquad \textbf{(5)}$$

The Freundlich adsorption isotherm data are shown in Fig.3. Where K_F is Freundlich constant (mg$^{1-1/n}$ l$^{1/n}$ g^{-1}), 1/n is the heterogeneity factor. K_F is roughly an indicator of the adsorption capacity and *n* of the adsorption intensity. The magnitude of the exponent *n* gives an indication of the favorability and capacity of the adsorbent/adsorbate system. Values $n > 1$ represent favorable adsorption conditions. In most cases the exponent between $1 < n < 10$ shows beneficial adsorption[23]. In the present study, since n lies between 1 and 10, it indicates the physical adsorption of methylene blues onto PSCFS. It can be concluded that from R^2 values in linear equation the were good for studying the adsorption of methylene blue dye onto PSCFS within the used concentration range but the fit with the Langmuir equation was comparably better. The isotherm parameters for the adsorption of methylene blue onto PSCFS are given in Table 1.

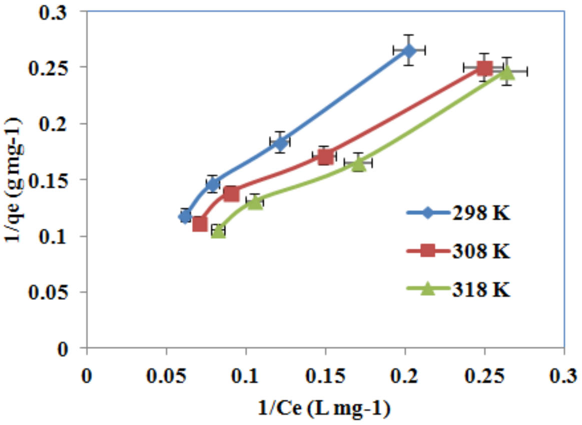

Fig.2. Langmuir plots for adsorption of MB by PSCFS.

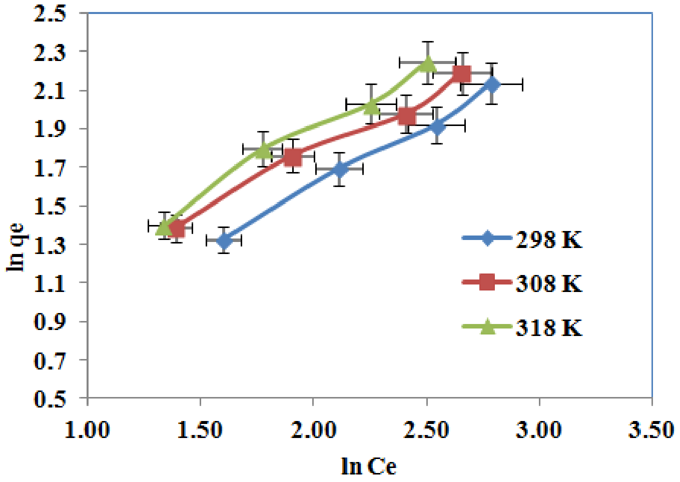

Fig.3. Freundlich plots for adsorption of MB by PSCFS.

The Dubinin-Kaganer-Radushkevick (DKR) equations is used to estimate the characteristic porosity of the adsorbent and the apparent energy of adsorption. The model is represented by the equation:

$$\ln q_e = \ln q_m - K_{DKR}\varepsilon^2 \qquad \textbf{(6)}$$

where q_e *is* amount of dye adsorbed per gram of PSCFS, q_{DKR} is isotherm constant related to degree of methlene blue (mg/g), K_{DKR} is a constant related to sorption energy(mol/kJ)^2, C_e *is* equilibrium concentration of dye (mg/L) and

$$\varepsilon = RT\ln(1+\frac{1}{C_e}) \qquad \textbf{(7)}$$

which is called as Polanyi Potential. A plot of ln *qe vs.* ε^2 yielding straight line confirms the model (Fig.4). The DKR constant can be determined from the intercept of the straight line graph. E(kJ/mol) mean free energy of adsorption per molecule of the adsorbate when it is transferred to the surface of the solid from infinity in the solution and can be computed by the relationship [24]:

$$E = \frac{1}{\sqrt{2K_{DKR}}} \qquad \textbf{(8)}$$

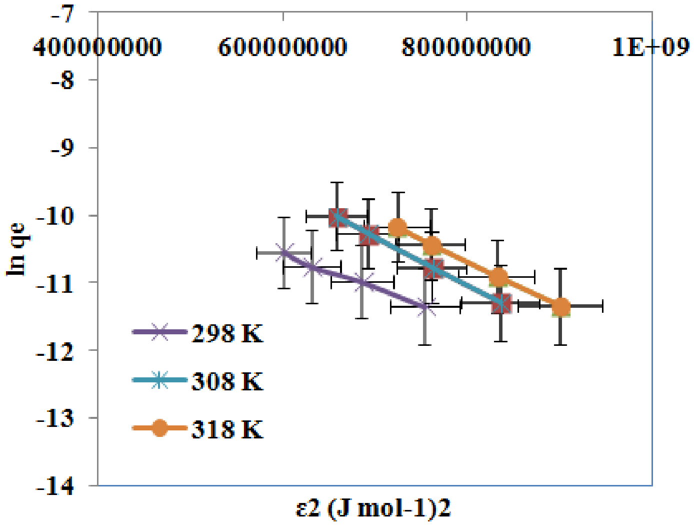

Fig.4. DKR adsorption isotherm plots for adsorption of MB onto PSCFS.

The DKR adsorption isotherm data are shown in Fig.4. The DKR parameters are listed in Table 1. As shown in Table 1, the *E* values lies in between 8.349-9.891 kJ/mol for dye sorption on PSCFS. These values indicate chemical adsorption by follow ion-exchange, in which the sorption energy lies within 8-16 kJ/mol [25].

The sorption capacity q_m in the DKR equation is found to be in between 8.219-9.509 mg/g which was less than the Langmuir adsorption capacity (15.480-21.692 mg/g) in differrent temperatures in the adsorption process. The R^2 values in table 1 for DKR equation are extremely high in investigated concentrations range which indicate complience adsorption data with DKR equations.

The Temkin model proposes into account the effects of the interaction of the adsorbate and the adsorbing species [26]. By ignoring the extremely low and large concentration values, the model assumes that the heat of adsorption (a function of temperature) of all of the molecules in the layer would decrease linearly rather than logarithmically with coverage due to adsorbate-adsorbent interactions [27], the equation is stated as follows:

$$q_e = \frac{RT}{b_T} \ln A_T + \frac{RT}{b_T} \ln C_e \tag{9}$$

where *b* Tempkin constant related to the heat of adsorption (kJ/mol), and A_T empirical Tempkin constant related to the equilibrium binding constant related to the maximum binding energy (L/mg). A plot of q_e versus ln C_e enables the determination of the isotherm constants A_T and b.

The Temkin adsorption isotherm data are shown in Fig.5.The constants A_T and b together with the R^2 values are shown in Table 1. Due to the low values isotherms constant, A_T, (0.527-0.723 L/g) and the values of R^2 (0.975-0.982), the data of equilibrium isotherms of MB onto PSCFS is poorly described by the Temkin model.

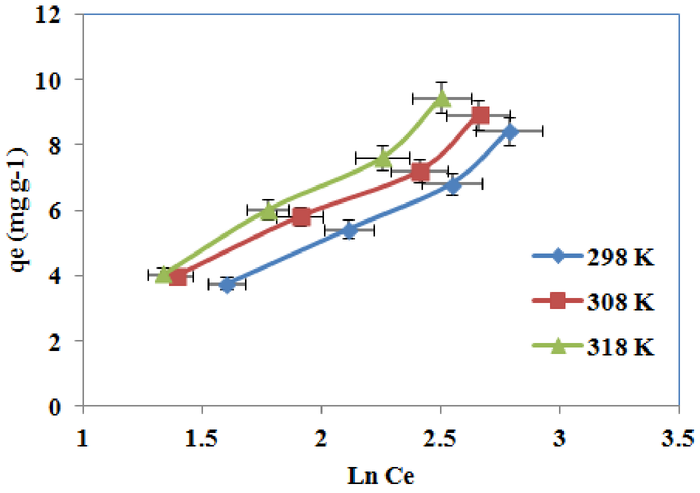

Fig.5. Temkin adsorption isotherm plots for adsorption of MB onto PSCFS.

Brunauer-Emmett-Teller (BET) isotherm is a theoretical equation, most widely applied in the gas-solid equilibrium systems [28]. It was developed to derive multilayer adsorption systems with relative pressure ranges from 0.05 to 0.30 corresponding to a monolayer coverage lying between 0.50 and 1.50. The linear form of BET equation can be written as follows:

$$\frac{C_e}{q_e(C_s - C_e)} = \frac{1}{q_m C_{BET}} + \frac{(C_{BET} - 1)}{q_m C_{BET}} \frac{C_e}{C_s} \tag{10}$$

where C_{BET}, C_s and q_m are the BET adsorption isotherm constant explaining the energy of interaction with surface (L/mg), adsorbate monolayer saturation concentration (mg/L), theoretical isotherm saturation capacity (mg/g), respectively. The values of C_{BET} and q_m were calculated from the slope and intercept of the linear plot $\frac{C_e}{q_e(C_s - C_e)}$ versus $\frac{C_e}{C_s}$.The BET adsorption isotherm data are shown in Fig.6. The Correlation coefficient and constans for BET isotherms are given in Table 2. Negative values for the BET isotherm constant (C_{BET}) indicate the inadequacy of the isotherm model to explain the adsorption process, since this constant is indicative of the surface binding energy [29]. The correlation coefficients (between 0.929-0.935) and low q_m values (between 1.438-1.621 mg/g) also support these results.

The Harkins-Jura adsorption isotherm accounts to multilayer adsorption and can be explained with the existence of heterogeneous pore distribution. The linear form of Harkins-Jura adsorption isotherm can be expressed as:

$$\frac{1}{q_e^2} = \frac{B_{HJ}}{A_{HJ}} - \frac{\log C_e}{A_{HJ}} \qquad \textbf{(11)}$$

A_{HJ} is Harkins-Jura isotherm parameter which accounts for multilayer adsorption and explains the existence of heterogeneous pore distribution, B_{HJ} is the isotherm constants [29]. The Harkins-Jura isotherm models for MB adsorption onto PSCFS are presented in Fig. 7 and the relevant isotherm parameters (Table 1) shows that the values of R^2 are located in the range of 0.904- 0.946. This result reveals that dye adsorption onto PSCFS is not support of the multilayer adsorption.

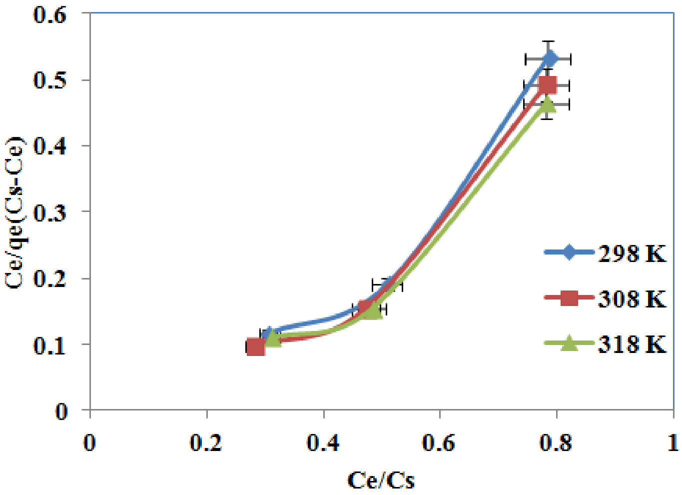

Fig.6. BET adsorption isotherm plots for adsorption of MB onto PSCFS.

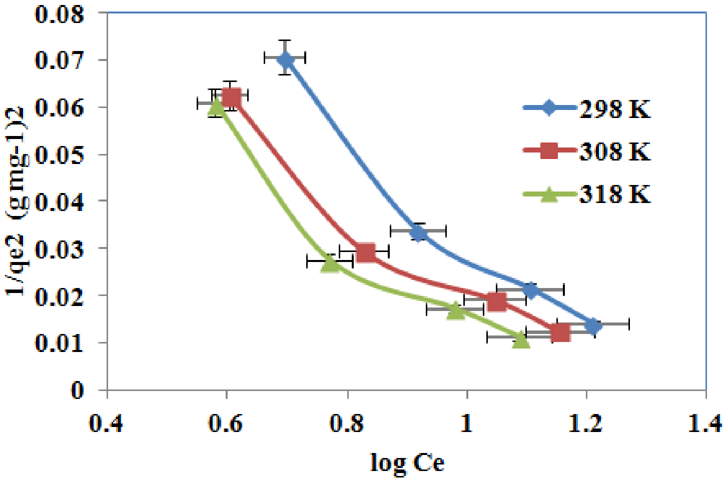

Fig.7. Harkins-Jura adsorption isotherm plots for adsorption of MB onto PSCFS.

The equation defining the Elovich model is based on a kinetic principle assuming that the adsorption sites increase exponentially with adsorption, which implies a multilayer adsorption [31]. The linear form of the Temkin isotherm equation is given as:

$$\ln \frac{q_e}{C_e} = \ln K_E q_m - \frac{q_e}{q_m} \qquad \textbf{(12)}$$

Where K_E is the Elovich equilibrium constant (L/mg) and q_m is the Elovich maximum adsorption capacity (mg/g). The Elovich isotherm models for MB adsorption onto PSCFS are shown in Fig. 8. The Elovich isotherm constants, K_E and q_m, as well as the coefficient of correlation, R^2, for the methylene blue compounds adsorption systems using PSCFS are obtained using the linear form of the equation (Table 1). In all cases, the Elovich isotherm exhibited higher coefficients of correlation, but lower than those obtained for other isotherms equations. In spite of the good correlation coefficients, the values of maximum adsorption capacity determined using the linear the Elovich equation (Table 1) are much higher than the experimental adsorbed amounts at equilibrium corresponding to the plateaus of the adsorption isotherms. This means that implies multilayer adsorption is not in agreement with the experiment in the studied concentration range. Therefore, the Elovich model is not enough to explain the adsorption isotherms of MB onto PSCFS.

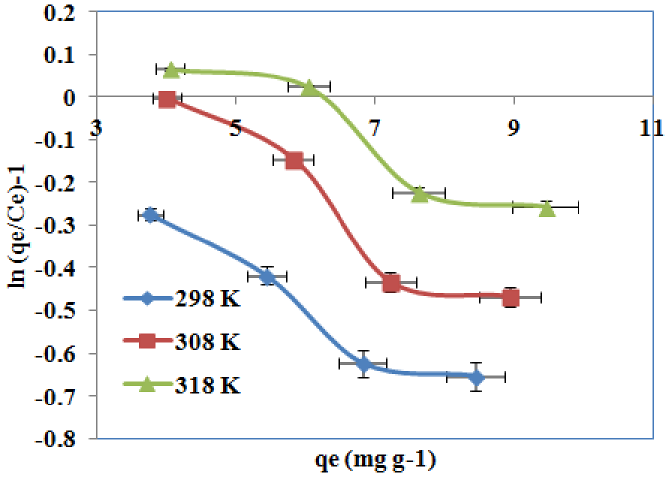

Fig.8. Elovich adsorption isotherm plots for adsorption of MB onto PSCFS**.**

Fowler-Guggenheim equation is an isotherm equation which takes the lateral interaction of the adsorbed molecules into account[32]. The linear form of the Fowler-Guggenheim eqution is shown as:

$$\ln\left[\frac{C_e(1-\theta)}{\theta}\right] = -\ln K_{FG} + \frac{2W\theta}{RT} \qquad \textbf{(13)}$$

Where K_{FG} is the Fowler-Guggenheim equilibrium constant (L/ mg), θ the fractional coverage and W is the interaction energy between adsorbed molecules (kJ/ mol). The Fowler-Guggenheim (FG) isotherm models for MB adsorption onto PSCFS are shown in Fig. 9. The FG isotherm constants, K_{FG} and W, as well as the coefficient of correlation, R^2, for the MB compounds adsorption systems using PSCFS are obtained using the linear form of the equation (Table 2). In this isotherms data, W is negative indicating that the interaction among adsorbed molecules is repulsive and therefore the heat of adsorption shows a decrease with loading [33].

Hill-de Boer equation describes mobile adsorption and lateral interaction among adsorbed molecules[34]. The linear form of the Hill-de Boer isotherm can be written as follows:

$$\ln\left[\frac{C_e(1-\theta)}{\theta}\right] - \frac{\theta}{1-\theta} = -\ln K_{HB} - \frac{K_1\theta}{RT} \qquad \textbf{(14)}$$

K_{HB} and K_1 can be determined by plotting $\ln\left[\frac{C_e(1-\theta)}{\theta} - \frac{\theta}{1-\theta}\right]$ versus θ. Where K_{HB} is the Hill-de Boer constant (L /mg), K_1 is the energetic constant of the interaction between adsorbed molecules (kJ/ mol). This isotherm graph is shown in fig. 10. Isotherms constants and correlation coefficient are given in table 2. As shown from Table 2, the value of the R^2 values was between 0.992-1.000, which are extremely high values fort he investigated range of concentrations. The values of K_1 is negative, indicating repulsive interaction among adsorbed molecules, and showing a decrease in the heat of adsorption with loading [35].

Frumkin isotherm, which takes into account interaction between the adsorbed species [36]. The linear form of this equation can be given as follows:

$$\ln\left[\left(\frac{\theta}{1-\theta}\right)\frac{1}{C_e}\right] = \ln K_{Fr} + 2a\theta \qquad \textbf{(15)}$$

Where the constant K_{Fr} is related to adsorption equilibrium, *a* is the interaction coefficient The parameters a and K_{Fr} are obtained from slope and intercept of the plot $\ln\left[\left(\frac{\theta}{1-\theta}\right)\frac{1}{C_e}\right]$ versus θ. The value of K_{Fr} constant in this equation is expresssed as follows:

$$\ln K_{Fr} = \frac{-\Delta G}{RT} \tag{16}$$

Table 1 Adsorption isotherm constants of two-parameter models for MB adsorption onto PSCFS

Isotherm models	**Parameters**	**Adsorbent matter**		
		298 K	**308 K**	**318 K**
Langmuir	q_m (mg/g)	16.475	15.480	21.692
	R_L	0.251-0.455	0.187-0.365	0.244-0.446
	K_L (L/mg)	0.060	0.087	0.062
	R^2	0.995	0.992	0.990
Freundlich	*n*	1.513	1.650	1.445
	K_F	1.315	1.753	1.661
	R^2	0.994	0.987	0.984
Dubinin-Kaganer-Radushkevich	*E* (kJ/mol)	9.891	8.349	8.704
	K_{DKR} (mol^2/kJ^2)	5.11x10^{-9}	7.17x10^{-9}	6.60x10^{-9}
	q_m (mg/g)	8.219	8.641	9.509
	R^2	0.993	0.999	0.999
Temkin model	A_T (L/mg)	0.527	0.723	0.659
	b_T (kJ/mol)	0.656	0.696	0.603
	R^2	0.976	0.975	0.982
BET model	n_{Hn}	1.498	1.633	1.498
	K_{Hn}	3.73x10^2	1.25x10^3	1.01x10^2
	R^2	0.994	0.987	0.984
Harkins-Jura model	A_{HJ}	9.259	11.415	10.695
	B_{HJ}	1.306	1.261	1.166
	R^2	0.946	0.929	0.904
Elovich model	K_E (L/g)	1.015	1.194	1.144
	q_m (mg/g)	11.574	9.756	14.819
	R^2	0.927	0.910	0.872

Frumkin isotherms graphs are given in figure 10 and isotherm constants and isotherm constans with regression coefficient are shown in table 2. The positive *a* parameter values indicate that there is attractive interaction between the adsorbed species [37]. The different a parameter values are attributed to differences in the orientation of the molecules. The ΔG values is changed in a narrow range with mean values -6.727, -6.106 and -6.678 kJ/mol for he adsorption methlene blue at different temperatures (298 K, 308 K and 318 K), respectively. The negative Δ*G* values means that the endothermic nature of the adsorption process [38].

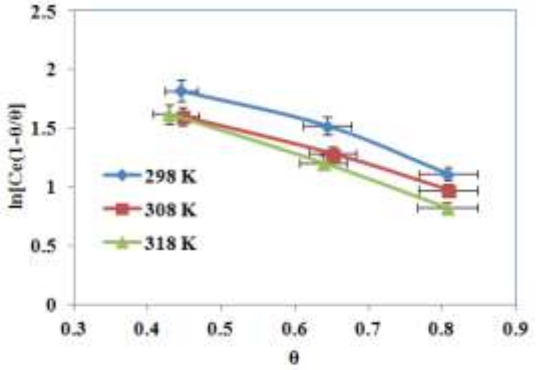

Fig.9. Fowler-Guggenheim adsorption isotherm plots for adsorption of MB onto PSCFS.

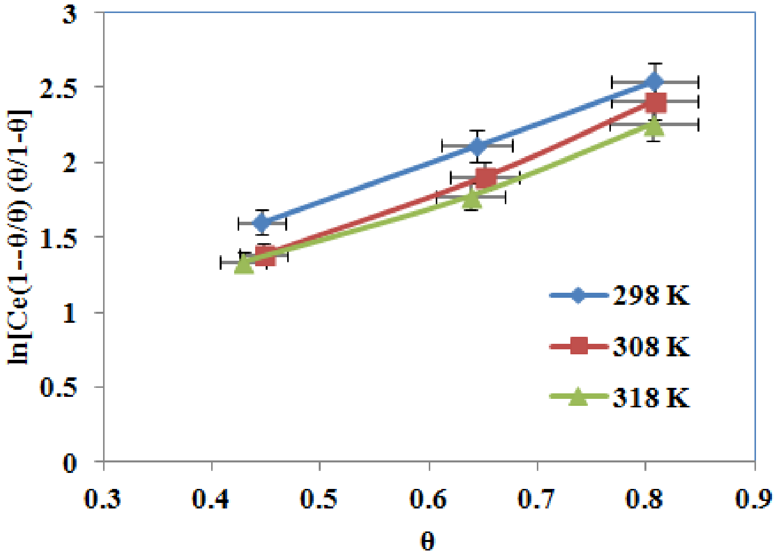

Fig.10. Frumkin adsorption isotherm plots for adsorption of Methylene Blue onto PSCFS.

Halsey isotherm describes condensation of a multilayer at a relatively large distance from the surface [39]. This equations are suitable for multilayer adsorption and the fitting of the experimental data to this equation attest to the heteroporous nature of the adsorbent.The Linear form of this equation is given as follow:

$$\log q_e = \frac{1}{n_H}\log K_H - \frac{1}{n_H}\log C_e \qquad \textbf{(17)}$$

The Halsey isotherm parameters are obtained from the plot of $\log q_e$ versus $\log C_e$. Where n_H and K_H are isotherm costants. Fig. 11 shows linear Halsey isotherms graph. The constants and correlation coefficients of the related equation are listed in table 2. The fitting of the Halsey isotherm equation was very high (R^2 =0.984-0.994), which is an indication of the heteroporosity of the PSCFS.

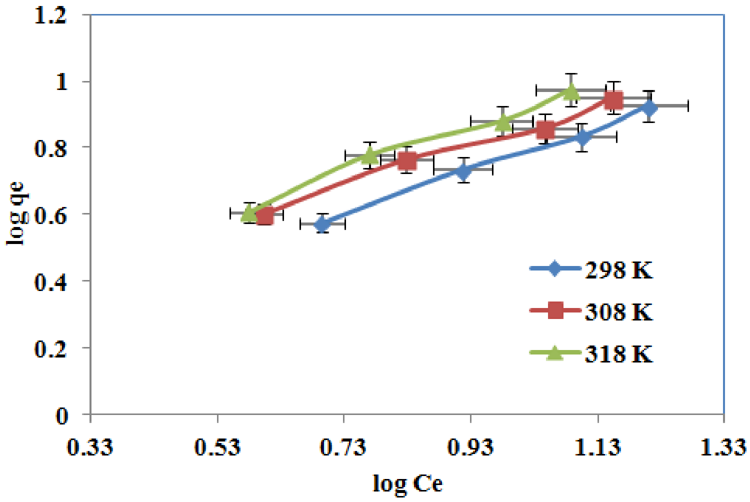

Fig.11. Halsey adsorption isotherm plots for adsorption of MB onto PSCFS.

The Henderson isotherm model studies the multilayer adsorption and the equilibrium data may be acceptably fitted by means of the following linearized equation that describes the heteroporous solids adsorption mechanisms [36]. The Linear form of this equation is given as follow:

$$\ln\left[-\ln(1-C_e)\right] = \ln K_{Hn} + n_{Hn}\ln q_e \qquad \textbf{(18)}$$

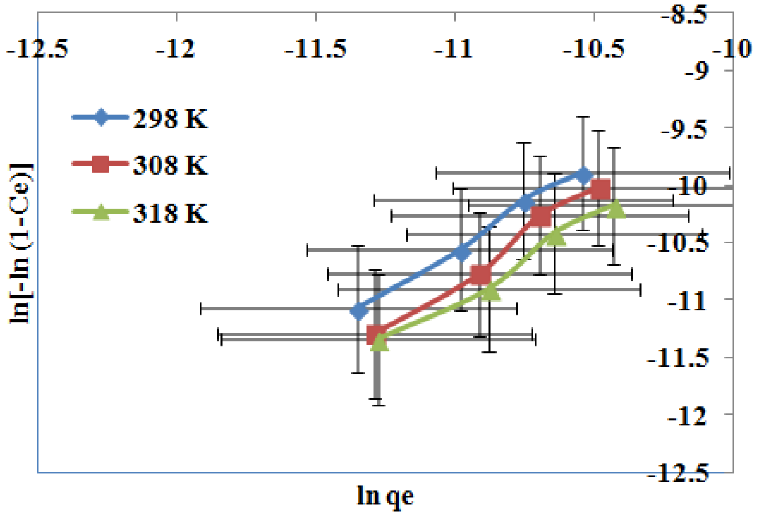

Fig.12. Henderson adsorption isotherm plots for adsorption of MB onto PSCFS.

Where K_{Hn} and n_{Hn} are known as Henderson constants. The plots of ln q_e against ln(-ln(1-C_e) are shown in Fig. 12 and the constant parameters obtained from this graph are given in table 2. The high correlation coefficient values (R^2=0.984-0.994) in this equation are shown heteroporous adsorption mechanisms.

Smith model ,like the Halsey and Henderson models, is concerned withadsorption on heterogenous surfaces In the this model, the adsorbed amount on the surface is subdivided into a bound and a normally condensed fraction. The bound fraction of adsorbate is on the inner or outer surface of the solid adsorbent by forces in excess of the normal forces for condensation. The normally condensed fraction may also have more than one condensed layer of adsorbate [40]. The linear form of this isotherms is as follow:

$$q_e = W_b - W \ln(1 - C_e) \qquad \textbf{(19)}$$

Where W and W_b are the constant parameters for the isotherm equation. The graphs of this isotherms are shown in fig. 13 and the constants and coorlation coefficients are given table 2. The high correlatin coefficient values (R^2) (between 0.981-0.992) indicate that the experimental data correspond to the Smith model in the tested concentration intervals.

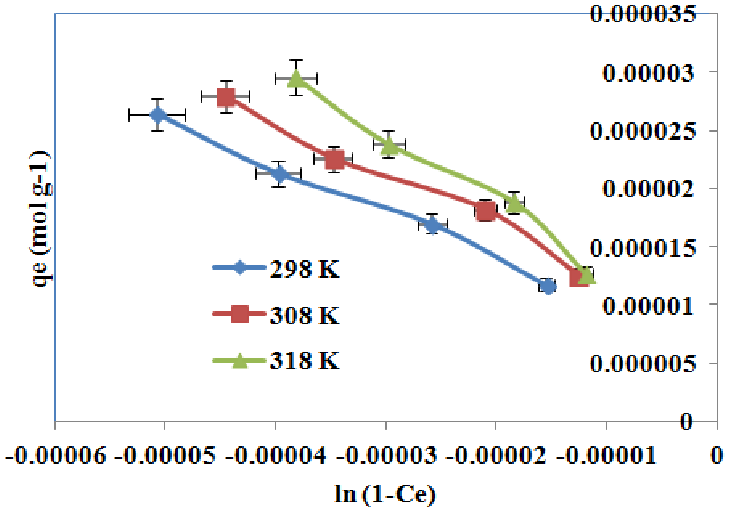

Fig.13. Smith adsorption isotherm plots for adsorption of MB onto PSCFS.

The model of an adsorption surface considered by Jovanovic is essentially the same as that considered by Langmuir, except that the allowance is made in the former for the surface binding vibrations of an adsorbed species [41]. In addition, the Jovanovic model considers the possibility of some mechanical contacts between the adsorbing and desorbing molecules[42].The linear form of this equation is given as:

$$\ln q_e = -K_J C_e + \ln q_m \qquad \textbf{(20)}$$

Where K_J (L/g) and q_m (mg/g) are Jovanovic model constants. The plots of this isotherms are given in fig. 14 and the data obtained from the isotherms are in table 2. The correlation coefficients in this isotherm data varies from 0.945-0.970. The data show that the accordance of the Jovanovic of experimental results is not very good.

The Scatchard plot analysis also called independent site oriented model was applied in order to obtain a comprehensive study on the affinity of binding sites and to analyse the result of the adsorption isotherm [43]. The linear form of this equation is given as:

$$\frac{q_e}{C_e} = -K_{Sc}q_e + K_{Sc}q_m \qquad \textbf{(21)}$$

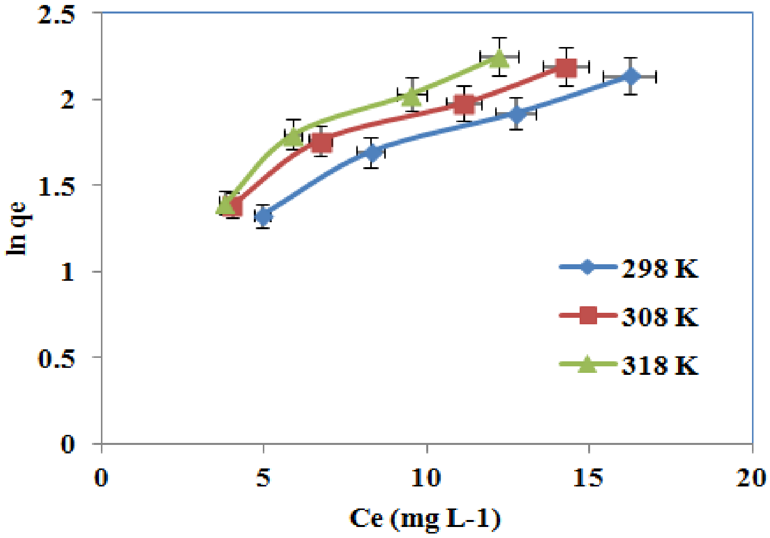

Fig.14. Jovanovic adsorption isotherm plots for adsorption of MB onto PSCFS.

Where K_{SC} and q_m are the Scatchard isotherm constants. The graphs of tis isotherms are shown in fig. 15 and data are given table 2. In this equation, if the graphs deviate from linearity, then the adsorbent consist of more than one type of binding site [43]. The regression values (R^2) varying from 0.873-0.922 indicate the deviation from the linearity of the data which means that PSCFS is contained more than one type of binding site.

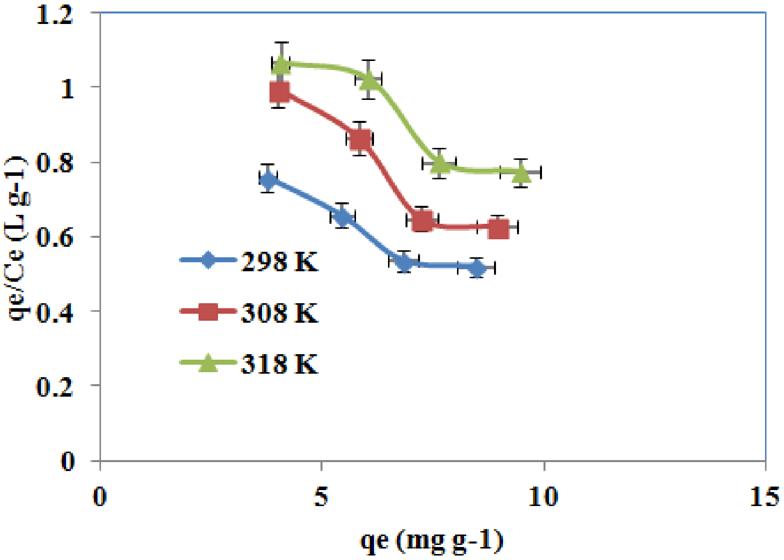

Fig.15. Scatchard adsorption isotherm plots for adsorption of MB onto PSCFS.

Table 2 Adsorption isotherm constants of two-parameter models for MB adsorption onto PSCFS

Isotherm models	**Parameters**	**Adsorbent matter**		
		298 K	**308 K**	**318 K**
Fowler-Guggenheim model	W (kJ/mol)	-2.409	-2.153	-2.597
	K_{FG} (L/mg)	-15.066	-10.854	-12.497
	R^2	0.979	0.996	0.999
Hill de Boer model	K_1(kJ/mol)	-6.455	-7.214	-6.410
	K_{HB}(L/g)	-1.549	-1.118	-1.312
	R^2	1.000	0.995	0.992
Frumkin model	ΔG(kJ/mol)	-6.727	-6.106	-6.678
	K_{FR} (L/g)	$6.64x10^{-2}$	$9.21x10^{-2}$	$8.00x10^{-2}$
	a	0.972	0.865	1.048
	R^2	0.979	0.996	0.999
Halsey model	K_H	0.661	0.396	0.480
	n_H	-1.513	-1.650	-1.445
	R^2	0.994	0.987	0.984
Henderson model	n_{Hn}	1.498	1.633	1.498
	K_{Hn}	$3.73x10^2$	$1.25x10^3$	$1.01x10^2$
	R^2	0.994	0.987	0.984
Smith model	W_B	$5.90x10^{-6}$	$7.43x10^{-6}$	$6.32x10^{-6}$
	W	0.401	0.456	0.607
	R^2	0.992	0.982	0.981
Jovanovic model	K_J (L/g)	$6.88x10^{-2}$	$7.36x10^{-2}$	$9.40x10^{-2}$
	q_m (mg/g)	2.837	3.202	3.096
	R^2	0.970	0.954	0.945
Scatchard	K_{Sc} (L/g)	$5.42x10^{-2}$	$8.11x10^{-2}$	$6.16x10^{-2}$
	q_m (mg/g)	17.530	16.160	21.677
	R^2	0.922	0.912	0.873

IV. Conclusions

The capacity of PSCFS for removing MB from water solutions was investigated, including equilibrium adsorption isotherms. Experiments were performed as a function of initial dye concentrations and examined the effect of temperature with time. From the experimental data, PSCFS has been found to be a low-capacity adsobent (q_m= 9.509 mg/g from DKR isotherms). Nevertheless, this material is used as an adsorbent to remove the methylene blue from aqueous solution. This adsorbent may be preferred due to its low cost and its use without any treatment. As seen in table 1 and table 2, the DKR isotherm provides a better fit with experimental data when compared to other isotherms. The values of R^2 for DKR and Langmuir models are almost close together but comparison of their maximum monolayer capacity show that DKR reveals a better agreement with experimental data. The value of q_m was 9.509 mg/g (at 318 K) which is more close to experimental capacity(about 8.400 mg/g 318 K) in comparison with corresponding Langmuir parameter (q_m) which is almost two and a half times (21.692 mg/g at 318 K) of the experimental capacity. The q_m values found in Bet, Jovanovic and Scatchard equations are not compatible with the experimental data as much as the DKR.

References

[1]. P. Marques, M. F. Rosa, H. M. Pinheiro, pH effects on the removal of Cu^{2+}, Cd^{2+} and Pb^{2+} from aqueous solution by waste brewery biomass, Bioprocess Engineering, 23(2), 2000, 135-141.

[2]. D. Ghosh, K.G. Bhattacharyya, Adsorption of methylene blue on kaolinite, *Applied Clay Science 20(6),* 2002, 295-300.

[3]. I. A.W. Tan, L. Ahmad, B. H. Hameed, (2008) Adsorption of basic dye on high-surface-area activated carbon prepared from coconut husk: equilibrium, kinetic and thermodynamic studies. *Journal of Hazardous Materials, 154(1-3),* 2008, 337-346.

[4]. A. K. Jain, V.K. Gupta, A. Bhatnagar, Utilization of industrial waste products as adsorbents for the removal of dyes, *Journal of Hazardous Materials, B101(1),* 2003, 31-42.

[5]. Y.S. Ho, G. McKay, Sorption of dyes and copper ions onto biosorbents, *Process Biochemistry, 38(7),* 2003, 1047-1061.

[6]. G. Akkaya, F. Guzel, Application of some domestic wastes as new low-cost biosorbents for removal of methylene blue: kinetic and equilibrium studies, *Chemical Engineering Communications, 201(4),* 2014, 557-578.

[7]. A. Ahmad, M. Rafatullah, O. Sulaiman, M. Ibrahim, R. Hashim, (2009) Scavenging behaviour of meranti sawdust in the removal of methylene blue from aqueous solution, *Journal of Hazardous Materials, 170(1),* 2009, 357-365.

[8]. L.W. Low, T.T. Teng, M. Rafatullah, N. Morad, B. Azahari, Adsorption studies of methylene blue and malachite green from aqueous solutions by pretreated lignocellulosic materials. *Separation* Science and Technology, 48(11), 2013, 1688-1698.

[9]. Z. M. Hussin, N. Talib, N.M. Hussin, M.A. Hanafiah, W.K. Khalir, Methylene blue adsorption onto NaOH modified durian leaf powder: isotherm and kinetic studies. *American Journal of Environmental Engineering, 5(3A),* 2015, 38-43.

[10]. H. Saygili, G. Akkaya Saygili, F. Güzel, (2014) Using grape pulp asa new alternative biosorbent for removal of a model basic dye, *Asia-Pacific Journal of Chemical Engineering, 9(2),* 2014, 214-225.

[11]. V.K. Thakur, M.K. Thakur, Recent advances in graft copolymerization and applications of chitosan: a review, *ACS Sustainable Chemistry and Engineering, 2(12),* 2014, 2637-2652.

[12]. M.S. Sajab, C.H. Chia, S. Zakaria, S.M. Jani, M.K. Ayob, K.L. Chee, P.S. Khiew, W. S. Chiu, Citric acid modified kenaf core fibres for removal of methylene blue from aqueous solution. *Bioresource Technology, 102(15),* 2011, 7237-7243.

[13]. D. Li, J. Yan, Z. Liu, Z. Liu, Adsorption kinetics studies for removal of methylene blue using activated carbon prepared from sugar beet pulp, *International Journal of Environmental Science and Technology, 13(7),* 2016, 1815-1822.

[14]. N. Jain, M.K. Dwivedi, A. Waskle, Adsorption of Methylene Blue Dye from Industrial Effluents Using Coal Fly Ash, *International Journal of Advanced Engineering Research and Science, 3(4),* 2016, 2349-6495.

[15]. **A. M. El-Wakil, W.M. Abou El-Maaty, A. A. Al-Ridha Oudah, (2015)** Methylene Blue Dye Removal from Aqueous Solution Using Several Solid Stationary Phases Prepared from Papyrus Plant, *Journal of Analitycal and Bioanalytical Techniques 13,* 2015,1-7.

[16]. N. Abdel-Ghani, G. El-Chaghaby, E. Zahran, Pentachlorophenol (PCP) adsorption from aqueous solution by activated carbons prepared from corn wastes, *International Journal of Environmental Science Technology, 12(1),* 2015, 211-222.

[17]. C, Namasivayam, R.T. Yamuna, (1995), Waste biogas residual slurry for the removal of Pb(II) from aqueous solution and radiator manufacturing industry wastewater, *Bioresource Technology, 52(5),* 1995, 125-131.

[18]. K.V. Kumar, S. Sivanesan, , (2006) Isotherm parameters for basic dyes onto activated carbon: Comparison of linear and non-linear method, *Journal of Hazardous Materials, B129(1-3),* 2006, 147-150.

[19]. G. Mckay, H.S. Blair, J. R. Gardiner, The adsorption of dyes onto chitin in fixed bed column and batch absorbers, Journal of Applied Polymer Science, 29(5), 1984, 1499-1514.

[20]. S.D. Khattri, M, Singh, Adsorption of basic dyes from aqueous solution by natural adsorbent. Indian Journal of Chemical Technology, 6(2), 1999, 112–116.

[21]. H.M.F. Freundlich, Over the adsorption in solution, *The Journal of Physical Chemistry, 57,*1906, 385-471.

[22]. A.W.Adamson, A.P. Gast, (1997) *Physical Chemistry of Surfaces* (sixth edition, Wiley- Interscience, New York, 1997).

[23]. A. M. Gamal, S.A. Abo Farha, H.B. Sallam, G.E.A. Mahmoud, L.F.M.Ismail, Kinetic Study and Equilibrium Isotherm Analysis of Reactive Dyes Adsorption onto Cotton Fiber. *Nature and Science, 8(11),* 2010, 95-110.

[24]. J.P. Hobson, Physical adsorption isotherms extending from ultra high vacuum to vapor pressure, *The Journal of physical chemistry, 73,*1969, 2720-2727.

[25]. Ö. Adnan, E.M.Öncü, A.S. Özcan, Kinetics, isotherm and thermodynamic studies of adsorption of Acid Blue 193 from aqueous solutions onto natural sepiolite, *Colloid and Surfaces A: Physicochemical and Engineering Aspects 277(1-3),* 2006, 90-97.

[26]. M.I. Tempkin, V. Pyzhev, Kinetics of ammonia synthesis on promoted iron catalyst, *Acta Physiochimica USSR 12,* 1940, 327-356.

[27]. C. Aharoni, M. Ungarish, Kinetics of activated chemisorption. Part 2. Theoretical Models, *Journal of Chemical Society. Faraday Transactions 1: Physical Chemistry in Condensed Phases, 73,* 1977, 456–464.

[28]. S. Bruanuer, S, P.H. Emmett, E. Teller, Adsorption of gases in multimolecular layers, *Journal American Chemical Society, 60,* 1938, 309–316.

[29]. K.R. Ramakrishna, T. Viraraghavan, Dye removal using low cost adsorbents, *Water Science and Technology, 36(2,3),* 1997, 189-196.

[30]. B.K. Suyamboo, R.S. Perumal, Equilibrium, Thermodynamic and Kinetic Studies on Adsorption of a Basic Dye by *Citrullus lanatus* Rind. Iranica Journal of Energy and Environment, 3(1), 2012, 23-34.

[31]. S.Y. Elovich, O.G. Larinov, Theory of adsorption from solutions of non electrolytes on solid (I) equation adsorption from solutions and the analysis of its simplest form, (II) verification of the equation of adsorption isotherm from solutions, *Izvestiya Akademii Nauk SSSR, Otdelenie Khimicheskikh Nauk2*(2), 1962, 209-216.

[32]. T. L. Hill, Statistical Mechanics of Multimolecular Adsorption II. Localized and mobile adsorption and absorption, *The Journal Chemical Physics 14(7),* 1946, 441-453.

[33]. Q. Hamdadoui, E. Naffrechoux, Modeling of adsorption isotherms of phenol and chlorophenols onto granular activated carbon Part I. Two-parameter models and equations allowing determination of thermodynamic parameters, *Journal of Hazardous Materials, 147(1-2),* 2007, 381-394.

[34]. J.H. De Boer, The Dynamical Character of Adsorption (Oxford University Press, Oxford, 1953).

[35]. N.S. Yousef, N. Farouq, R., Hazzaa, Adsorption kinetics and isotherms for the removal of nickel ions from aqueous solutions by an ion-exchange resin: application of two and three parameter isotherm models, *Desalination and Water Treatment, 57,* 2016, 21925-21938.

[36]. C. A. Başar, Applicability of the various adsorption models of three dyes adsorption onto activated carbon prepared waste apricot, *Journal Hazardous Materials 135(1-3),* 2006, 232-241.

[37]. C. Quan, G. Khoe, D. Bagster, Adsorption of sodium lauryl sulfate onto arsenic-bearing ferrihydrite. *Water Resource, 35(2),* 2001, 478-484.

[38]. P.K. Malik, Use of activated carbons prepared from sawdust and rice-husk for adsorption of acid dyes: a case study of Acid Yellow 36, *Dyes Pigments 56(3),* 2003, 239-249.

[39]. G. Halsey, (1948) Physical adsorption on nonuniform surface. *The Journal Chemical Physics, 16(10),* 1948, 931-937.

[40]. S.E. Smith, (1947) The sorption of water vapor by high polymers, *Journal of the American Chemical Society,* 69, 1947, 646-651.

[41]. D.S. Jovanovic, Physical adsorption of gases I: isotherms for monolayer and multilayer adsorption, *Colloid Polymer Science, 235,* 1969, 1203-1214.

[42]. H. Shahbeig, N. Bagheri, S.A. Ghorbanian, A. Hallajisani, S. Poorkarimi, A New Adsorption Isotherm Model of Aqueous Solutions on Granular Activated Carbon, *World Journal of Modelling and Simulation, 9(4),* 2013, 243- 254.

[43]. T.S. Anirudhan, P.S. Suchithra, (2012) Equilibrium, Kinetic and Thermodynamic Modeling for The Adsorption of Heavy Metals Onto Chemically Modified Hydrotalcite, *Indian Journal of Chemical Technology 17(4),* 2012, 247-259.